



Preparation and characterization of a novel Al¹⁸F–NOTA–BZA conjugate for melanin-targeted imaging of malignant melanoma



Chih-Chao Chang^a, Chih-Hsien Chang^{a,b}, Yi-Hsuan Lo^a, Ming-Hsien Lin^c, Chih-Chieh Shen^d, Ren-Shyan Liu^{a,e,f}, Hsin-Ell Wang^{a,*}, Chuan-Lin Chen^{a,*}

^a Department of Biomedical Imaging and Radiological Sciences, National Yang-Ming University, No. 155, Li-Nong St., Sec. 2, Pei-tou, Taipei 11221, Taiwan

^b Isotope Application Division, Institute of Nuclear Energy Research, Taoyuan, Taiwan

^c Department of Nuclear Medicine, Taipei City Hospital, Zhongxiao Branch, Taipei, Taiwan

^d Department of Nuclear Medicine, Cheng Hsin General Hospital, Taipei, Taiwan

^e Molecular and Genetic Imaging Core/Taiwan Mouse Clinic, National Comprehensive Mouse Phenotyping and Drug Testing Center, Taipei, Taiwan

^f National PET/Cyclotron Center and Department of Nuclear Medicine, Taipei Veterans General Hospital, Taipei, Taiwan

ARTICLE INFO

Article history:

Received 19 January 2016

Revised 7 June 2016

Accepted 9 June 2016

Available online 9 June 2016

Keywords:

NOTA

Melanoma

Benzamide

Al–F complex

Positron emission tomography

ABSTRACT

Melanin is an attractive target for the diagnosis and treatment of malignant melanoma. Previous studies have demonstrated the specific binding ability of benzamide moiety to melanin. In this study, we developed a novel ¹⁸F-labeled NOTA–benzamide conjugate, Al¹⁸F–NOTA–BZA, which can be synthesized in 30 min with a radiochemical yield of 20–35% and a radiochemical purity of >95%. Al¹⁸F–NOTA–BZA is highly hydrophilic (log*P* = –1.96) and shows good in vitro stability. Intravenous administration of Al¹⁸F–NOTA–BZA in two melanoma-bearing mouse models revealed highly specific uptake in B16F0 melanotic melanoma (6.67 ± 0.91 and 1.50 ± 0.26% ID/g at 15 and 120 min p.i., respectively), but not in A375 amelanotic melanoma (0.87 ± 0.21 and 0.24 ± 0.09% ID/g at 15 and 120 min p.i., respectively). The clearance from most normal tissues was fast. A microPET scan of Al¹⁸F–NOTA–BZA-injected mice also displayed high-contrast tumor images as compared with normal organs. Owing to the favorable in vivo distribution of Al¹⁸F–NOTA–BZA after intravenous administration, the estimated absorption dose was low in all normal organs and tissues. The melanin-specific binding ability, sustained tumor retention, fast normal tissues clearance and the low projected human dosimetry supported that Al¹⁸F–NOTA–BZA is a very promising melanin-specific PET probe for melanin-positive melanoma.

© 2016 Elsevier Ltd. All rights reserved.

Melanoma is one of the most lethal forms of skin cancer.¹ It ranks fifth in men and seventh in women as the most common cancer in the United States.² The incidence of melanoma has increased significantly over the past 3 decades, doubling almost every decade.³ The prognosis and the patient's survival depend on the clinical stage of the disease at the time of diagnosis.⁴

A key feature of melanoma is the extensive melanin expression in most tumor cells. The entirely nonpigmented form is very uncommon in melanoma. Melanotic tumors represent over 90% of all malignant melanomas.⁵ Melanotic melanoma develops from genetically altered neoplastic melanocytes that contain extensive melanin, thus making it a very attractive target for diagnostic imaging and therapy.⁶ Melanin is a group of biopolymers that contain indole units with carboxyl functionalities and phenolic

hydroxyl groups,⁷ with the capability of binding many different types of compounds.⁸

Several melanin-targeted PET and single-photon emission computed tomography (SPECT) probes containing benzamide or nicotinamide moiety have been successfully developed (Fig. 1 and Table 1), such as *N*-(2-diethylaminoethyl)-4-¹²³I-iodobenzamide (¹²³I-IBZA),^{9,10} *N*-(2-diethylaminoethyl)-4-¹⁸F-fluorobenzamide (¹⁸F-FBZA),¹¹ *N*-(2-diethylaminoethyl)-4-(4-fluorobenzamido)-5-¹²³I-iodo-2-methoxybenzamide (¹²³I-MIP-1145),¹² ¹⁸F-6-fluoro-*N*-((2-(diethylamino)ethyl)pyridine-3-carboxamide (¹⁸F-MELO50),^{13,14} ¹²³I-*N*-(2-(diethylamino)ethyl)-5-iodonicotinamide (¹²³I-MELO08),¹⁵ ^{123/131}I-6-chloro-*N*-(4-((2-(diethylamino)ethyl)carbamoyl)-2-iodo-5-methoxyphenyl)nicotinamide (^{123/131}I-Iochlonicotinamide),¹⁶ ⁶⁸Ga-labeled *N*-(2-diethylaminoethyl)benzamide derivative (⁶⁸Ga-SCN–NOTA–BZA),¹⁷ ⁶⁸Ga-labeled DOTA–benzamide derivative (⁶⁸Ga-SCN–DOTA–PCA)¹⁸ and the radioiodinated phenylacetamide and its homologue (^{123/131}I-IHPA/IHPP).¹⁹ However, most benzamide/nicotinamide-based probes show relatively high accumulation in some normal organs, particularly the liver.

* Corresponding authors. Tel.: +886 2 28267215; fax: +886 2 28201095 (H.-E.W.); tel.: +886 2 28267062; fax: +886 2 28201095 (C.-L.C.).

E-mail addresses: hewang@ym.edu.tw (H.-E. Wang), clchen2@ym.edu.tw (C.-L. Chen).

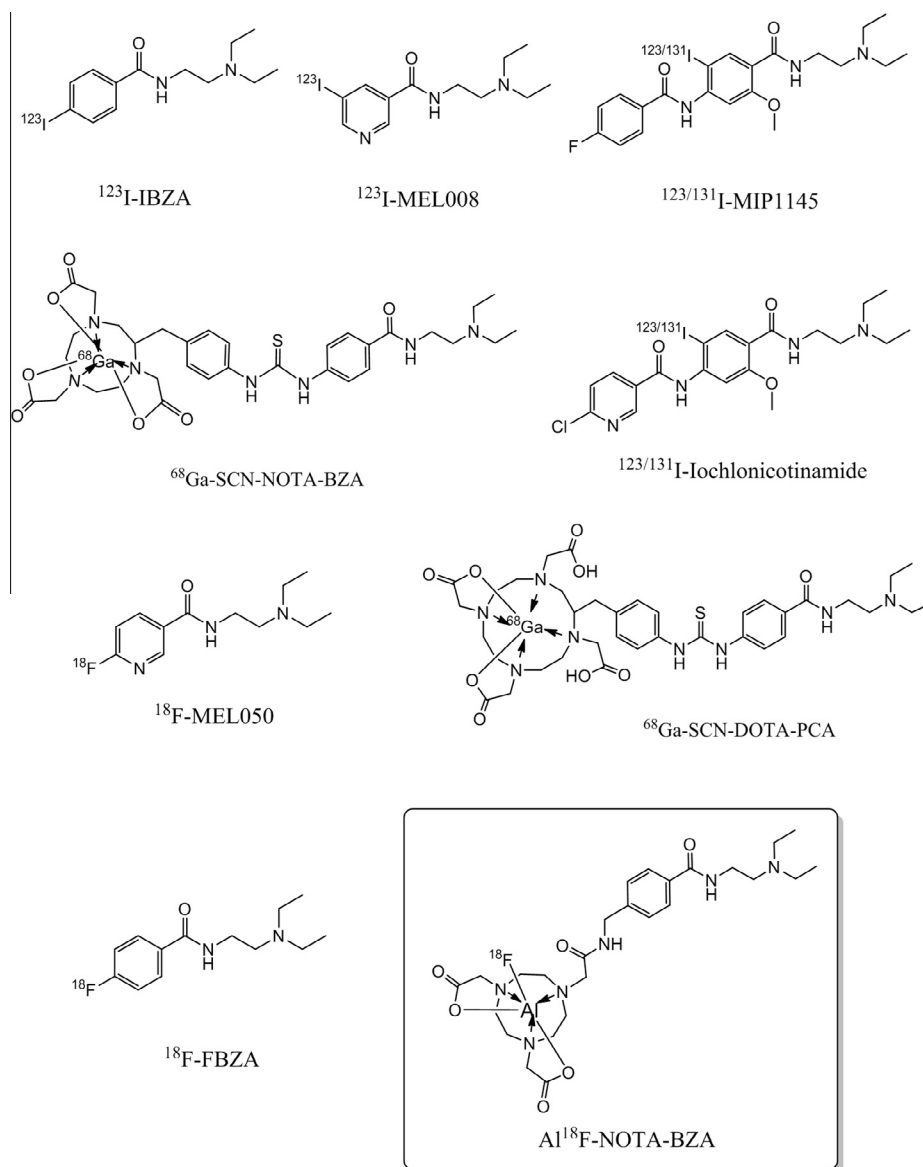


Figure 1. Chemical structure of melanin-targeting melanoma probes developed for imaging and/or targeted radionuclide therapy of melanoma and Al^{18}F -NOTA-BZA.

Among various positron-emitting isotopes, ^{18}F (half-life, 110 min) has nearly ideal properties for PET, such as low positron energy, lack of side emissions, and a suitable half-life. The routinely used nucleophilic ^{18}F fluorination requires multistep procedures including repeated azeotropic distillation, radiolabeling at high temperature in an organic solvent containing base catalyst, and the evaporation of organic solvent.²⁰ For example, the synthesis of ^{18}F -FBZA is usually conducted via conjugation of ^{18}F -*N*-succinimidyl-4-fluorobenzoate (^{18}F -SFB) to the primary amino group of *N,N*-diethylethylenediamine (DEDA), which requires a multistep synthesis and is time-consuming and laborious.⁴

Recently, several pioneering studies on one-step ^{18}F -labeling methods have been reported.^{20–22} Fluoride binds strongly to aluminum, which can then form a stable chelate with NOTA in water.²³ A one-step radiofluorination via Al^{18}F complex may greatly reduce the total synthesis time and enable the kit-production of ^{18}F -labeled complex. The water-compatible reaction is ideal for the incorporation of ^{18}F -fluoride into biologically active ligands, especially those biomolecules that are soluble only in water. A validated lyophilized kit that enables rapid and

reliable labeling of a ligand by a simple addition of $^{18}\text{F}^-$ in saline, then a brief heating step, followed by a rapid and simple purification process, would make the Al^{18}F radiofluorination of molecules more compatible with the already established good manufacturing practices (GMP) applied for the preparation of $^{99\text{m}}\text{Tc}$ -agents.²⁴

In this study, we developed a novel NOTA-benzamide derivative, Al^{18}F -NOTA-BZA, by forming Al^{18}F complex (Fig. 1), and we performed the biological characterizations in two melanoma mouse models to demonstrate it as a promising PET probe for targeted melanin imaging. All the procedures of chemical syntheses (compounds **2**, **3**, **4**, **5**, **6** and **7a**), the Al^{18}F radiofluorination (**7b**), and the chemical and biological characterizations are detailed in [Supplementary materials](#).

The authentic standard **7a** and radiotracer **7b** were prepared from NOTA-conjugated precursor NOTA-BZA (**6**), which was synthesized from 4-(aminomethyl)benzoic acid **1** through a five-step procedure (Scheme 1). Compound **2** was produced by the reaction of **1** with $(\text{Boc})_2\text{O}$ in 1 N NaOH at room temperature for 8 h, followed by further purification by silica gel column chromatography

Table 1

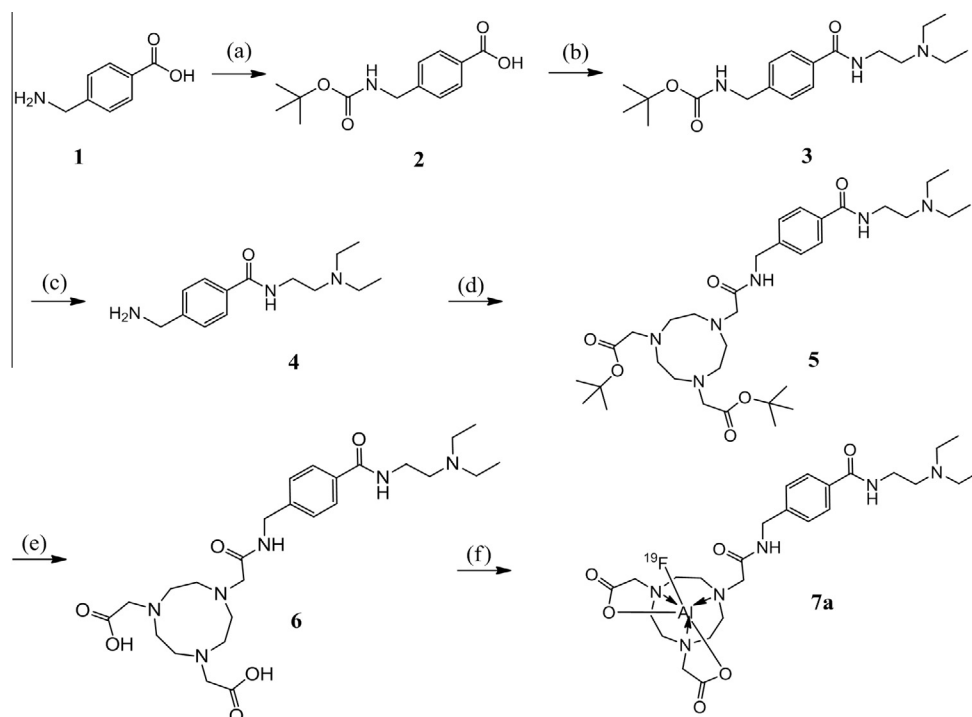
Comparison of several melanin-targeted PET and SPECT probes containing benzamide or nicotinamide moiety

Radiotracer	Lipophilicity (log <i>P</i>)	Tumor model	Tumor uptake, [†] T/M and [†] T/L (at 1 h p.i.)	Reference
¹²³ I-IBZA	1.44	B16	5.5% ID/g, T/M = 6.0, T/L < 1	10
¹⁸ F-FBZA	1.70	B16F10	6.5% ID/g, T/M = 5.2, T/L = 0.7	11
¹⁸ F-MEL050	0.94	B16F0	8.4% ID/g, T/M = ND, T/L = ND	14
^{123/131} I-MIP-1145	ND	SKMEL-3	3.8% ID/g, T/M = 2.7, T/L = 0.5	12
¹²³ I-MEL008	1.55	B16F0	6.2% ID/g, T/M = ND, T/L = 3.1	15
¹³¹ I-lochlo-nicotinamide	0.67	B16F0	13.5% ID/g, T/M = 17.3, T/L = 3.4	16
¹³¹ I-IHPA/IHPP	−0.38/0.07	B16F0	10.1/10.9% ID/g, T/M = 19.0/21.1, T/L = 6.2/6.8	19
⁶⁸ Ga-SCN-NOTA-BZA	−3.25	B16F10	1.6% ID/g, T/M = 8.0, T/L = 2.3	17
⁶⁸ Ga-SCN-DOTA-PCA	−3.70	B16F10	2.6% ID/g, T/M = 8.7, T/L = 0.8	18
Al ¹⁸ F-NOTA-BZA	−1.96	B16F0	3.4% ID/g, T/M = 13.8, T/L = 4.4	

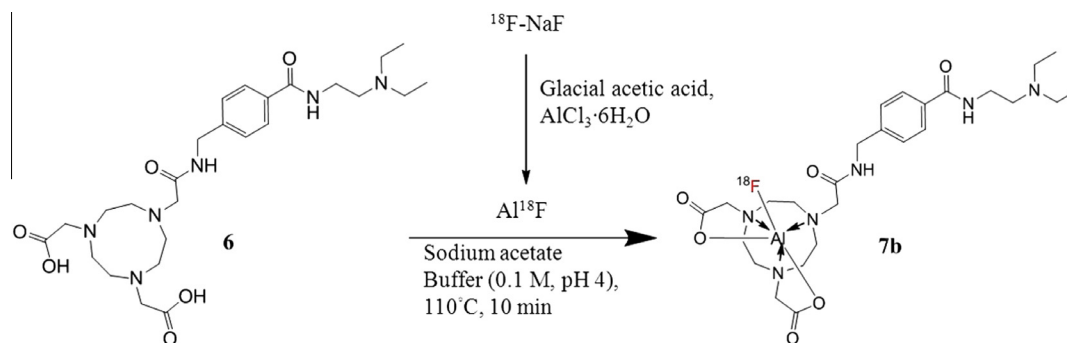
[†] T/M and T/L were the tumor-to-muscle and tumor-to-liver ratios.

at 78% yield. Compound **3** was synthesized using **2** and anhydrous potassium carbonate dissolved in anhydrous THF; then DEDA, HOBt and EDC were added at ambient temperature for 16 h. The mixture was filtered, washed and purified by silica gel column chromatography at 80% yield. The *tert*-butyloxycarbonyl protecting group (BOC group) of **3** was cleaved by TFA in CH₂Cl₂, giving purified compound **4**. Compound **4** was obtained by silica gel column purification (yield: 75%) and then conjugated with HBTU, HOBt, and NOTA(*t*-Bu)₂ in CH₂Cl₂ using DIPEA as a base at ambient temperature to afford compound **5** (yield: 55%). Precursor **6** was obtained by removing the *t*-Bu group of **5** with TFA in CH₂Cl₂ at ambient temperature for 24 h. Al¹⁹F-NOTA-BZA **7a** was produced by the reaction of **6** with AlCl₃ and NaF solution in sodium acetate buffer (1 M, pH 3.5) at 100 °C for 1 h, followed by further purification by an HLB cartridge at 60% yield. The analytical HPLC was conducted using a Hypersil ODS column with a gradient elution (solvent A: 0.1% TFA in water, solvent B: 0.1% TFA in acetonitrile. Gradient elution 0–30 min: 100–70% A, 0–30% B; flow rate, 1 mL/min; UV (nm): λ₂₅₄; retention time, 17.6 min).

Radiosynthesis of the title complex Al¹⁸F-NOTA-BZA (**7b**) was shown in Scheme 2. Al¹⁸F complex was prepared by mixing ¹⁸F-fluoride and AlCl₃ stock solution in 0.1 M sodium acetate buffer (pH 4) at ambient temperature. The prepared Al¹⁸F was reacted with NOTA-BZA to give Al¹⁸F-NOTA-BZA (**7b**) with a labeling efficiency of 30–50% (Fig. 2A). The purified Al¹⁸F-NOTA-BZA was obtained after HLB cartridge purification with a radiochemical purity >95% (Fig. 2B). The identity of Al¹⁸F-NOTA-BZA was confirmed by the nonradioactive authentic compound **7a** (Al¹⁹F-NOTA-BZA) using analytical HPLC (Fig. 2C). The overall radiochemical yield was about 20–35% (decay corrected). The synthesis time was about 40 min from the end of bombardment (EOB), including the process of purification and formulation. The specific activity at the end of synthesis was 60–80 GBq/μmol. The analytical HPLC was conducted using a Hypersil ODS column with a gradient elution (solvent A: 0.1% TFA in water, solvent B: 0.1% TFA in acetonitrile, 0–30 min: 0–30% B; flow rate, 1 mL/min; UV (nm): λ₂₅₄; retention time, 18.5 min). The aluminum fluoride method eliminates the drying



Scheme 1. Chemical synthesis of precursor (**6**) and authentic Al¹⁹F-NOTA-BZA (**7a**). Reagents and conditions: (a) (Boc)₂O, 1 N NaOH, anhydrous THF, ambient temperature, 8 h; (b) DEDA, HOBt, EDC, K₂CO₃, anhydrous THF, ambient temperature, 24 h; (c) TFA, anhydrous CH₂Cl₂, ambient temperature, 3 h; (d) NOTA(*t*-Bu)₂, HBTU, HOBt, DIPEA, ambient temperature, 16 h; (e) TFA, anhydrous CH₂Cl₂, ambient temperature, 24 h; (f) AlCl₃, NaOAc buffer (1.0 M, pH 3.5), NaF, 100 °C, 2 h.



Scheme 2. Preparation of Al¹⁸F complexing agent and chelation with NOTA-BZA to obtain Al¹⁸F-NOTA-BZA (**7b**).

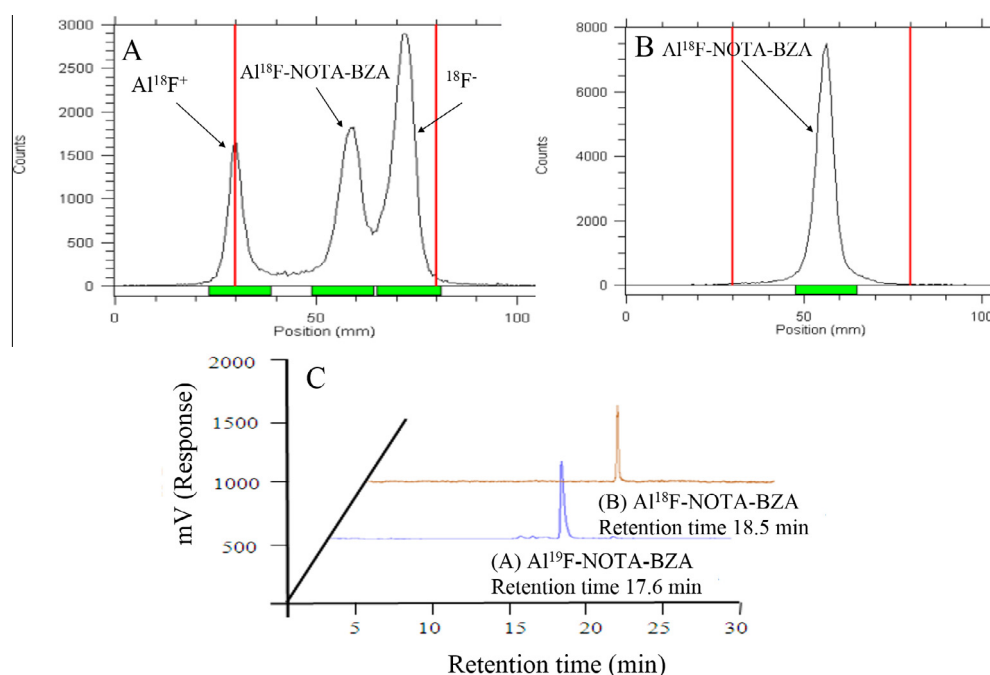


Figure 2. Radio instant thin-layer chromatograms of (A) reaction mixture, and (B) the purified Al¹⁸F-NOTA-BZA (ITLC-SG plate, developing agent: 0.05 M Na₂CO₃, radiochemical purity >95%). (C) The HPLC chromatograms of authentic Al¹⁹F-NOTA-BZA (UV-peak, λ₂₅₄, retention time 17.6 min, blue line), and purified Al¹⁸F-NOTA-BZA product (radio peak, retention time 18.5 min, brown line).

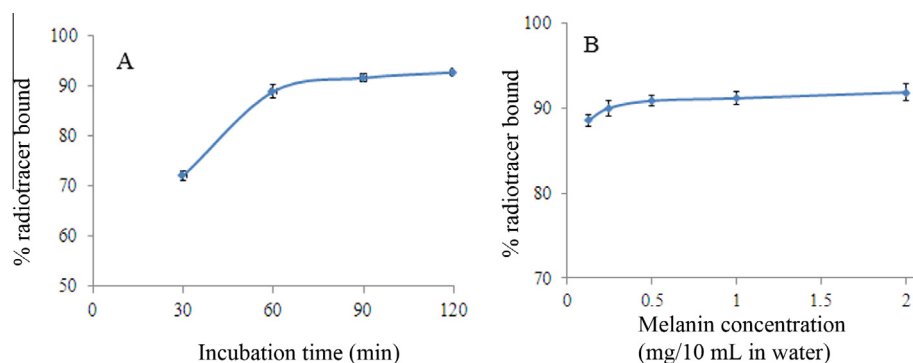


Figure 3. In vitro binding of Al¹⁸F-NOTA-BZA to synthetic melanin. (A) Effect of incubation time (30, 60, 90 and 120 min) at 37 °C. (B) Effect of melanin concentration (0.125, 0.25, 0.5, 1.0 and 2.0 mg/10 mL) for 60 min of incubation at 37 °C.

step from the labeling procedure, which is a major advantage as compared with conventional ¹⁸F-labeling methods.

Partition coefficient is generally considered an index of the lipophilicity of the probes. To determine the lipophilicity of

Al¹⁸F-NOTA-BZA, the radiotracer was added to a mixture of 1-octanol and phosphate buffer saline (PBS; pH 7.4), and the mixture was vigorously vortexed for 5 min. After subsequent centrifugation at 3000 rpm for 5 min, a sample of 100 μL was taken

from each phase and assayed for radioactivity with a gamma counter. A log *P* of -1.96 ± 0.14 revealed that Al¹⁸F-NOTA-BZA is more hydrophilic compared with those compounds reported in the literature, e.g., ¹²³I-IBZA (1.44), ¹⁸F-FBZA (1.70),⁴ and our previously reported compound ¹²³I-lochlonicotinamide (0.67)¹⁶ and ¹²³I-IHPA/IHPP ($-0.38/0.07$).¹⁹

The in vitro serum stability was evaluated by the incubation of 3.7 MBq of Al¹⁸F-NOTA-BZA in 1 mL of PBS and human serum at 37 °C. The radiochemical purities of Al¹⁸F-NOTA-BZA in PBS and human serum were both still >95% after 120 min of incubation as determined by the chromatographic method (ITLC-SG plate, developing agent 0.05 M Na₂CO₃), and exhibited a very good serum stability in vitro.

To assess the binding affinity of Al¹⁸F-NOTA-BZA to synthetic melanin, 0.74 MBq of this radiotracer was added into an aqueous melanin suspension (0.5 mg/10 mL). The mixture was vortexed intermittently for 30, 60, 90 and 120 min at 37 °C. The binding of Al¹⁸F-NOTA-BZA to melanin was rapid initially (72% after a 30-min incubation), plateaued at 60 min of incubation (90%), and remained high till 120 min of incubation (93%, Fig. 3A). In another study, the binding of Al¹⁸F-NOTA-BZA to various concentrations of melanin suspension was determined. About 0.74 MBq of Al¹⁸F-NOTA-BZA was mixed with 0.125, 0.25, 0.5, 1 and 2 mg/10 mL of synthetic melanin suspension and vortexed intermittently for 60 min at 37 °C. The bound ratio of Al¹⁸F-NOTA-BZA was almost the same for the melanin concentration, which ranged from 0.125 mg/10 mL (88%) to 2 mg/10 mL (92%) after 60 min of incubation (Fig. 3B). Our studies show that the binding of Al¹⁸F-NOTA-BZA to melanin is dependent on both the melanin concentration and the incubation time.

In vitro cellular uptake studies of Al¹⁸F-NOTA-BZA in B16F0 melanoma cells and A375 amelanotic melanoma cells were conducted. The B16F0 cell line is high melanin expressing, while the A375 cell line is non melanin expressing. An aliquot of Al¹⁸F-NOTA-BZA was added into each well and incubated at 37 °C for various time periods (15, 30, 60 and 120 min). A rapid and appreciable uptake in B16F0 melanoma cells ($1.13 \pm 0.06\%$ AD/10⁶ cells after 15 min of incubation, Fig. 4) was observed, followed by a gradual increase till 120 min of incubation ($1.64 \pm 0.06\%$ AD/10⁶ cells, Fig. 4). Although the high hydrophilicity did not appreciably interfere with the binding affinity of Al¹⁸F-NOTA-BZA to melanin, it may retard the transportation of this tracer through the cell membrane via diffusion and thus reduce the in vitro cellular uptake compared with those radiohalogenated probes with lower hydrophilicity reported in our previous studies.^{16,19} The uptake in amelanotic A375 melanoma cells, as expected, was very low ($0.24 \pm 0.02\%$ AD/10⁶ cells at 15 min, $0.18 \pm 0.02\%$ AD/10⁶ cells at

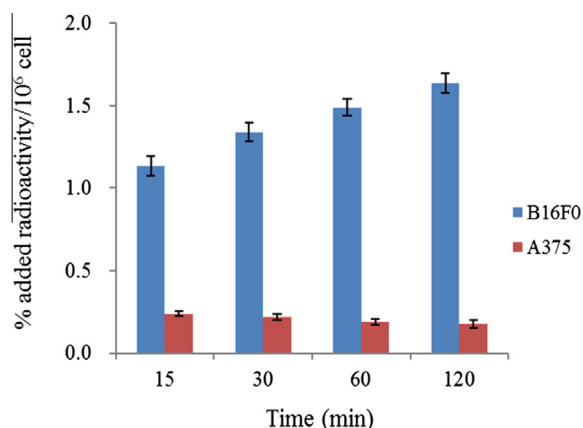


Figure 4. In vitro cellular uptake of Al¹⁸F-NOTA-BZA in B16F0 and A375 cells. Data are expressed as mean ± SD, with each data point representing triplicate study.

Table 2

Biodistribution of Al¹⁸F-NOTA-BZA in C57BL/6 mice bearing B16F0 tumor after iv injection of 3.7 MBq Al¹⁸F-NOTA-BZA. Values were presented as% ID/g (mean ± SD, n = 3 at each time point)

Organ	0.25 h	0.5 h	1 h	2 h
Blood	3.92 ± 0.88	1.21 ± 0.26	0.72 ± 0.13	0.26 ± 0.09
Heart	1.25 ± 0.11	0.89 ± 0.10	0.39 ± 0.06	0.24 ± 0.06
Lung	1.69 ± 0.34	1.18 ± 0.29	0.50 ± 0.11	0.22 ± 0.05
Liver	1.97 ± 0.32	1.24 ± 0.32	0.79 ± 0.12	0.29 ± 0.08
Stomach	1.85 ± 0.29	1.33 ± 0.22	0.67 ± 0.12	0.26 ± 0.07
S.Int	1.53 ± 0.34	1.05 ± 0.15	0.65 ± 0.14	0.32 ± 0.06
L.Int	1.42 ± 0.21	1.11 ± 0.21	0.57 ± 0.11	0.30 ± 0.04
Spleen	1.34 ± 0.23	0.71 ± 0.15	0.52 ± 0.14	0.23 ± 0.07
Pancreas	1.29 ± 0.29	0.81 ± 0.19	0.51 ± 0.11	0.17 ± 0.04
Muscle	0.86 ± 0.12	0.44 ± 0.07	0.25 ± 0.04	0.10 ± 0.03
Bone	0.94 ± 0.18	0.78 ± 0.10	0.68 ± 0.18	0.39 ± 0.10
Tumor	6.67 ± 0.91	4.48 ± 0.98	3.40 ± 0.41	1.52 ± 0.30
Brain	0.20 ± 0.02	0.12 ± 0.01	0.09 ± 0.01	0.06 ± 0.01
Kidney	7.31 ± 1.90	5.51 ± 1.13	4.36 ± 0.73	2.24 ± 0.48
Eyeball	3.07 ± 0.56	1.79 ± 0.44	1.17 ± 0.23	0.68 ± 0.11
Urine	340.4 ± 55.9	175.1 ± 38.9	101.6 ± 24.5	39.1 ± 13.5
Feces	0.53 ± 0.17	0.61 ± 0.20	0.58 ± 0.17	0.53 ± 0.16
<i>Uptake ratio</i>				
Tumor-to-muscle	7.70 ± 1.15	10.2 ± 1.72	13.8 ± 2.07	16.4 ± 2.55
Tumor-to-blood	1.76 ± 0.49	3.75 ± 0.69	4.78 ± 0.83	5.96 ± 0.81
Tumor-to-liver	3.45 ± 0.76	3.65 ± 0.47	4.35 ± 0.79	5.34 ± 0.61

Table 3

Biodistribution of Al¹⁸F-NOTA-BZA in BALB/c nude mice bearing A375 tumor after iv injection of 3.7 MBq Al¹⁸F-NOTA-BZA. Values were presented as% ID/g (mean ± SD, n = 3 at each time point)

Organ	0.25 h	0.5 h	1 h	2 h
Blood	3.10 ± 0.84	1.15 ± 0.32	0.45 ± 0.12	0.21 ± 0.06
Heart	0.83 ± 0.12	0.75 ± 0.15	0.34 ± 0.11	0.13 ± 0.04
Lung	0.85 ± 0.15	0.61 ± 0.11	0.30 ± 0.08	0.19 ± 0.07
Liver	1.34 ± 0.35	0.81 ± 0.22	0.52 ± 0.19	0.31 ± 0.09
Stomach	1.00 ± 0.22	0.65 ± 0.18	0.27 ± 0.09	0.16 ± 0.06
S.int	0.75 ± 0.11	0.64 ± 0.10	0.43 ± 0.12	0.22 ± 0.07
L.int	0.78 ± 0.13	0.72 ± 0.11	0.39 ± 0.09	0.26 ± 0.09
Spleen	0.77 ± 0.10	0.66 ± 0.12	0.31 ± 0.09	0.24 ± 0.07
Pancreas	0.70 ± 0.11	0.49 ± 0.10	0.26 ± 0.08	0.19 ± 0.06
Muscle	0.79 ± 0.25	0.42 ± 0.10	0.28 ± 0.08	0.16 ± 0.03
Bone	0.76 ± 0.15	0.53 ± 0.11	0.48 ± 0.13	0.23 ± 0.08
Tumor	0.87 ± 0.21	0.55 ± 0.17	0.37 ± 0.11	0.24 ± 0.09
Brain	0.11 ± 0.02	0.09 ± 0.01	0.07 ± 0.01	0.05 ± 0.02
Kidney	6.91 ± 1.57	5.08 ± 1.26	2.28 ± 0.65	1.34 ± 0.36
Eyeball	0.68 ± 0.14	0.51 ± 0.12	0.34 ± 0.09	0.21 ± 0.08
Urine	198.6 ± 71.4	115.8 ± 28.0	71.3 ± 16.8	21.7 ± 6.74
Feces	0.43 ± 0.12	0.66 ± 0.15	0.73 ± 0.14	0.92 ± 0.22
<i>Uptake ratio</i>				
Tumor-to-muscle	1.17 ± 0.35	1.28 ± 0.28	1.32 ± 0.29	1.50 ± 0.30
Tumor-to-blood	0.28 ± 0.10	0.48 ± 0.17	0.69 ± 0.13	1.16 ± 0.23
Tumor-to-liver	0.69 ± 0.26	0.70 ± 0.29	0.72 ± 0.15	0.77 ± 0.10

120 min of incubation). A 9-fold higher uptake of Al¹⁸F-NOTA-BZA in melanotic B16F0 cells than that in amelanotic A375 cells after 120 min of incubation indicated that Al¹⁸F-NOTA-BZA uptake is associated with melanin.

The biodistribution of Al¹⁸F-NOTA-BZA was performed in C57BL/6 mice bearing B16F0 murine melanoma and in BALB/c nude mice bearing A375 human amelanotic melanoma. After intravenous injection of Al¹⁸F-NOTA-BZA into B16F0 melanoma mice, a rapid and high uptake in high-melanin-expressing B16F0 melanoma ($6.67 \pm 0.91\%$ ID/g at 15 min p.i.) was observed, accompanied by a slower clearance ($1.50 \pm 0.26\%$ ID/g at 120 min p.i.) compared with most normal tissues (Table 2). The relatively sustained radioactivity retention in tumor rendered favorable tumor-to-normal tissue ratios for tumor detection. The tumor-to-muscle and tumor-to-liver ratios (7.70, 3.45 and 16.40, 5.34 at 15 and 120 min p.i., respectively) kept increasing with time. In addition, the bony uptake was low in both mouse models, indicating that

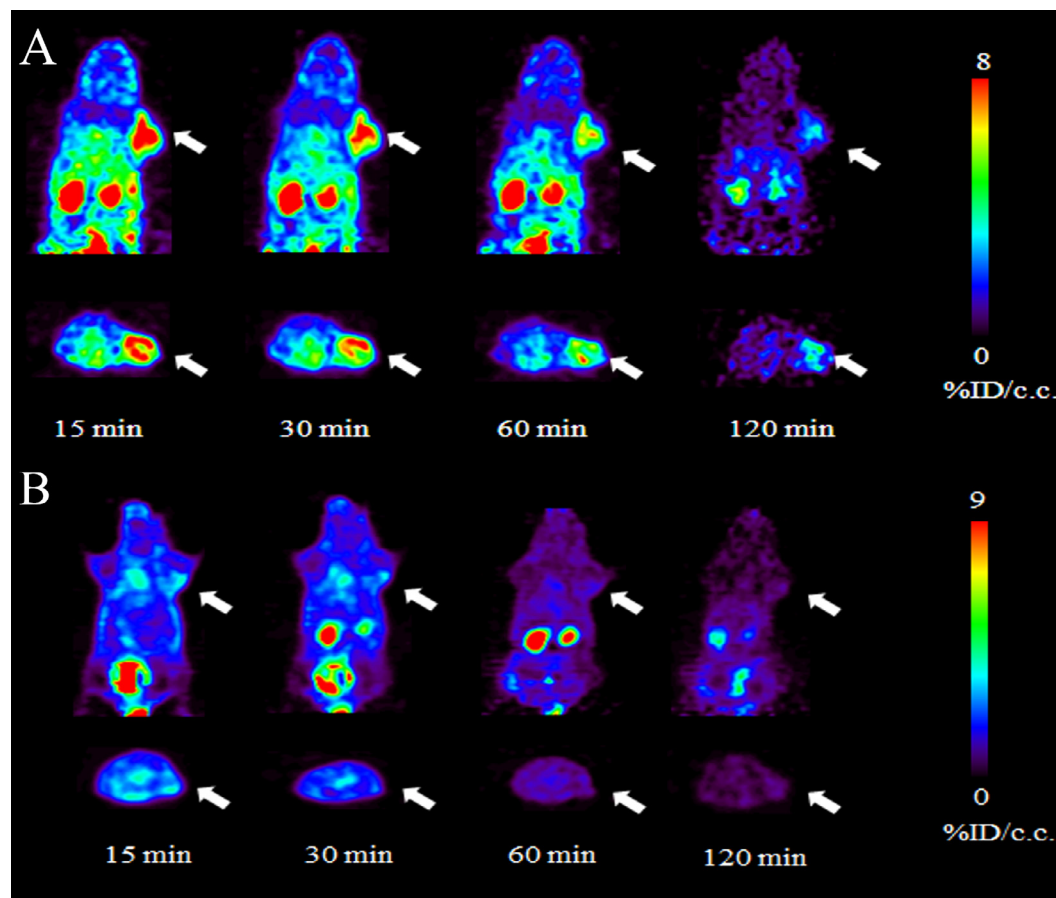


Figure 5. Representative coronal (top) and transaxial (bottom) Al^{18}F -NOTA-BZA microPET images of (A) C57BL/6 mice bearing B16F0 murine melanoma, and (B) BALB/c nude mice bearing A375 human amelanotic melanoma. Static microPET images were performed at 0.25, 0, 5, 1 and 2 h post-intravenous injection of approximately 3.7 MBq of Al^{18}F -NOTA-BZA. Arrows indicate tumors.

the Al^{18}F -NOTA complex was stable, without appreciable defluorination in vivo. A rapid radioactivity accumulation in the kidney and extremely high radioactivity observed in the urine suggested that Al^{18}F -NOTA-BZA and its radioactive metabolites are excreted mainly via the urinary system. The high hydrophilicity (low $\log P$ value) of Al^{18}F -NOTA-BZA enables its fast clearance from most normal tissues and thus improves the tumor-to-normal tissue ratios. In A375 amelanotic melanoma-bearing BALB/c nude mice, however, the tumor uptake was very low (0.87 ± 0.21 , 0.55 ± 0.17 , 0.37 ± 0.11 and $0.24 \pm 0.09\%$ ID/g at 15, 30, 60 and 120 min p.i., respectively, Table 3). The results of biodistribution studies clearly demonstrated the high targeting specificity of Al^{18}F -NOTA-BZA to melanin.

In addition to the biodistribution study, a microPET scan was also performed post-intravenous injection of Al^{18}F -NOTA-BZA in two melanoma mouse models. A high uptake in B16F0 melanoma was observed at 15 min p.i., and persisted till 120 min p.i. The B16F0 tumors can be clearly delineated with good tumor-to-background contrast within 120 min postinjection (Fig. 5A), whereas the A375 amelanotic melanoma in the BALB/c nude mouse was barely visualized (Fig. 5B). A rapid radioactivity accumulation in the urine indicated that Al^{18}F -NOTA-BZA was excreted mainly through renal routes in both mouse models; this was consistent with the observations of the biodistribution study. The results of microPET imaging demonstrated the rapid and specific targeting of Al^{18}F -NOTA-BZA to melanotic melanoma in a tumor mouse model.

The radiation-absorbed dose projections after the administration of Al^{18}F -NOTA-BZA to humans were calculated based on the residence time of several source organs in B16F0 tumor-bearing

Table 4
Radiation dose estimates for Al^{18}F -NOTA-BZA in humans

	Estimated dose ^a (mSv/MBq)
Organ	Al^{18}F -NOTA-BZA
Adrenals	$8.84\text{E} - 03$
Brain	$2.13\text{E} - 03$
Breasts	$7.50\text{E} - 03$
Gallbladder wall	$9.50\text{E} - 03$
LLI wall	$1.01\text{E} - 02$
Small intestine	$1.10\text{E} - 02$
Stomach wall	$8.89\text{E} - 03$
ULI wall	$1.04\text{E} - 02$
Heart wall	$5.75\text{E} - 03$
Kidneys	$1.06\text{E} - 02$
Liver	$4.79\text{E} - 03$
Lungs	$4.62\text{E} - 03$
Muscle	$5.02\text{E} - 03$
Ovaries	$1.03\text{E} - 02$
Pancreas	$5.78\text{E} - 03$
Red marrow	$7.68\text{E} - 03$
Osteogenic cells	$1.33\text{E} - 02$
Skin	$6.37\text{E} - 03$
Spleen	$5.37\text{E} - 03$
Testes	$8.52\text{E} - 03$
Thymus	$8.20\text{E} - 03$
Thyroid	$8.40\text{E} - 03$
Urinary bladder wall	$1.03\text{E} - 02$
Uterus	$1.08\text{E} - 02$
Total body	$7.92\text{E} - 03$
Effective dose	$9.01\text{E} - 03$

^a Radiation-absorbed dose projections in humans were determined from residence times for Al^{18}F -NOTA-BZA in C57BL/6 mice and were calculated using the OLINDA/EXM version 1.1 computer program.

Table 5
Radiation dose comparison of Al¹⁸F–NOTA–BZA with previously reported melanin-targeted probes in humans

Radiotracer	Liver	Kidneys	Urinary bladder wall	Small intestine	ULI wall	Tumor	Reference
Al ¹⁸ F–NOTA–BZA	0.48	1.06	1.03	1.10	1.04	185	
¹³¹ I-IHPA	11.9	17.0	49.2	50.9	49.2	3420	19
¹³¹ I-IHPP	12.2	16.9	48.8	51.3	49.6	3620	19
¹³¹ I-BA52	130	30.0	66	310	464	1220	25

Radiation-absorbed dose projections in humans were calculated using the OLINDA program. Values were presented as 1×10^{-2} mSv/MBq.

* Assuming a tumor mass of 10 g. Values were presented as 1×10^{-2} mGy/MBq.

C57BL/6 mice. The organ equivalent dose estimation for humans was shown in Table 4. The estimated absorption dose of the critical normal organs (liver, kidney, small intestine and upper large intestine wall) was in the range of only 0.005–0.01 mSv/MBq (Table 5). The doses given to these organs by Al¹⁸F–NOTA–BZA were much lower than those by ¹³¹I-BA52 reported in a clinical trial (Mier et al.)²⁵ and ¹³¹I-IHPA/IHPP reported in our previous study.¹⁹ Our newly developed Al¹⁸F–NOTA–BZA, with a pharmacodynamics of rapid melanoma accumulation and fast normal tissues clearance owing to its high hydrophilicity, displays a very low radiation burden to all normal tissues calculated by the OLINDA program when used for melanin-targeting PET imaging in humans. The radiation dosimetry presented here will be useful in the application of Al¹⁸F–NOTA–BZA for Investigational New Drug (IND) research.

In conclusion, we reported the synthesis with in vitro and in vivo characterizations of Al¹⁸F–NOTA–BZA as a melanin-specific PET probe in melanoma animal models. Al¹⁸F–NOTA–BZA can be rapidly prepared with ¹⁸F-fluoride via Al¹⁸F intermediate within 30 min with an accepted radiochemical yield (20–35%) and high radiochemical purity (>95%). The biodistribution and microPET studies of Al¹⁸F–NOTA–BZA in a B16F0 melanoma mouse model showed highly specific melanin-associated tissue accumulation. The results of this study suggest that Al¹⁸F–NOTA–BZA, a novel ¹⁸F labeled NOTA–benzamide derivative, is a promising and low-radiation-burden PET probe for melanin-specific imaging of melanin-positive melanoma.

Acknowledgements

This study was supported by grants from National Science Council Taiwan (NSC 101-2314-B-010-044-MY3), Taipei City Hospital, Zhongxiao Branch, Taiwan, and Cheng Hsin General Hospital, Taiwan (102F218C08). We thank the staff of National PET and Cyclotron Center in Taipei Veterans General Hospital, who kindly provided excellent technical assistance. Molecular and Genetic Imaging Core/Taiwan Mouse Clinic, National Comprehensive Mouse Phenotyping and Drug Testing Center, Taipei, Taiwan, is also gratefully acknowledged.

Supplementary data

Supplementary data associated with this article can be found, in the online version, at <http://dx.doi.org/10.1016/j.bmcl.2016.06.022>.

References and notes

- Rigel, D. S. *Arch. Dermatol.* **2010**, *146*, 318.
- Siegel, R.; Ma, J. M.; Zou, Z. H.; Jemal, A. *CA Cancer J. Clin.* **2014**, *64*, 9.
- Jennings, L.; Murphy, G. M. *Br. J. Dermatol.* **2009**, *161*, 496.
- Garg, S.; Kothari, K.; Thopate, S. R.; Doke, A. K.; Garg, P. K. *Bioconjugate Chem.* **2009**, *20*, 583.
- Koch, S. E.; Lange, J. R. *J. Am. Acad. Dermatol.* **2000**, *42*, 731.
- Sulaimon, S. S.; Kitchell, B. E. *Vet. Dermatol.* **2003**, *14*, 57.
- Prota, G. *Pigment Cell Res.* **2000**, *13*, 283.
- Dadachova, E.; Casadevall, A. *Future Oncol.* **2005**, *1*, 541.
- Michelot, J. M.; Moreau, M. F.; Veyre, A. J.; Bonafous, J. F.; Bacin, F. J.; Madelmont, J. C.; Bussiere, F.; Souteyrand, P. A.; Mauclair, L. P.; Chossat, F. M., et al. *J. Nucl. Med.* **1993**, *34*, 1260.
- Nicholl, C.; Mohammed, A.; Hull, W. E.; Bubeck, B.; Eisenhut, M. *J. Nucl. Med.* **1997**, *38*, 127.
- Ren, G.; Miao, Z.; Liu, H.; Jiang, L.; Limpa-Amara, N.; Mahmood, A.; Gambhir, S. S.; Cheng, Z. *J. Nucl. Med.* **2009**, *50*, 1692.
- Joyal, J. L.; Barrett, J. A.; Marquis, J. C.; Chen, J.; Hillier, S. M.; Maresca, K. P.; Boyd, M.; Gage, K.; Nimmagadda, S.; Kronauge, J. F.; Friebe, M.; Dinkelborg, L.; Stubbs, J. B.; Stabin, M. G.; Mairs, R.; Pomper, M. G.; Babich, J. W. *Cancer Res.* **2010**, *70*, 4045.
- Greguric, I.; Taylor, S. R.; Denoyer, D.; Ballantyne, P.; Berghofer, P.; Roselt, P.; Pham, T. Q.; Mattner, F.; Bourdier, T.; Neels, O. C.; Dorow, D. S.; Loc'h, C.; Hicks, R. J.; Katsifis, A. *J. Med. Chem.* **2009**, *52*, 5299.
- Denoyer, D.; Greguric, I.; Roselt, P.; Neels, O. C.; Aide, N.; Taylor, S. R.; Katsifis, A.; Dorow, D. S.; Hicks, R. J. *J. Nucl. Med.* **2010**, *51*, 441.
- Liu, X.; Pham, T. Q.; Berghofer, P.; Chapman, J.; Greguric, I.; Mitchell, P.; Mattner, F.; Loc'h, C.; Katsifis, A. *Nucl. Med. Biol.* **2008**, *35*, 769.
- Chang, C. C.; Chang, C. H.; Shen, C. C.; Chen, C. L.; Liu, R. S.; Lin, M. H.; Wang, H. E. *Bioorg. Med. Chem.* **2015**, *23*, 2261.
- Kim, H. J.; Kim, D. Y.; Park, J. H.; Yang, S. D.; Hur, M. G.; Min, J. J.; Yu, K. H. *Bioorg. Med. Chem.* **2012**, *20*, 4915.
- Kim, H. J.; Kim, D. Y.; Park, J. H.; Yang, S. D.; Hur, M. G.; Min, J. J.; Yu, K. H. *Bioorg. Med. Chem. Lett.* **2012**, *22*, 5288.
- Chang, C. C.; Chang, C. H.; Shen, C. C.; Chen, C. L.; Liu, R. S.; Lin, M. H.; Wang, H. E. *Eur. J. Pharm. Sci.* **2016**, *81*, 201.
- Laverman, P.; McBride, W. J.; Sharkey, R. M.; Eek, A.; Joosten, L.; Oyen, W. J.; Goldenberg, D. M.; Boerman, O. C. *J. Nucl. Med.* **2010**, *51*, 454.
- McBride, W. J.; D'Souza, C. A.; Sharkey, R. M.; Karacay, H.; Rossi, E. A.; Chang, C. H.; Goldenberg, D. M. *Bioconjugate Chem.* **2010**, *21*, 1331.
- McBride, W. J.; Sharkey, R. M.; Karacay, H.; D'Souza, C. A.; Rossi, E. A.; Laverman, P.; Chang, C. H.; Boerman, O. C.; Goldenberg, D. M. *J. Nucl. Med.* **2009**, *50*, 991.
- McBride, W. J.; Sharkey, R. M.; Goldenberg, D. M. *EJNMMI Res.* **2013**, *3*, 36.
- McBride, W. J.; D'Souza, C. A.; Karacay, H.; Sharkey, R. M.; Goldenberg, D. M. *Bioconjugate Chem.* **2012**, *23*, 538.
- Mier, W.; Kratochwil, C.; Hassel, J. C.; Giesel, F. L.; Beijer, B.; Babich, J. W.; Friebe, M.; Eisenhut, M.; Enk, A.; Haberkorn, U. *J. Nucl. Med.* **2014**, *55*, 9.